

13th International Conference on Greenhouse Gas Control Technologies, GHGT-13, 14-18
November 2016, Lausanne, Switzerland

Investigation of the Cooling System of a Membrane-Based Post-Combustion Process

Li Zhao^{a,*}, Alexander Otto^a, Martin Robinius^a, Detlef Stolten^{a,b}

^a*Institute of Energy and Climate Research – Electrochemical Process Engineering (IEK-3),
Forschungszentrum Jülich, D-52425 Jülich, Germany*

^b*Chair of Fuel Cells, RWTH Aachen University, D-52056 Aachen, Germany*

Abstract

This paper investigates post-combustion capture in coal-fired power plants equipped with gas separation membranes. Simulations are conducted with the process engineering software, Aspen Plus®, with its Exchanger Design and Rating (EDR) tool utilized for heat exchanger design. The reference power plant chosen for the investigation is the Reference Power Plant North Rhine-Westphalia (RPP-NRW) in Germany.

The Polyactive® membrane developed by the project partner, Helmholtz Zentrum Geesthacht, was used in the simulation. Because the membrane has different properties at different working temperatures in order to reach a higher degree of selectivity and less energy consumption, the flue gas should be cooled to 25 °C. This results in an efficient cooling system for the capture process, which merits further development.

A rigorous heat exchanger design leads to a significant increase in the pressure drops at each heat exchanger and hence the pressure ratio required by the compression machines. The energy penalty of the membrane CCS system for 57% and 76% degrees of CO₂ separation was increased from 4.7%-pts to 5.3%-pts and 7%-pts to 8.3%-pts, respectively, after implementing the rigorous heat exchanger design.

© 2017 Published by Elsevier Ltd. This is an open access article under the CC BY-NC-ND license (<http://creativecommons.org/licenses/by-nc-nd/4.0/>).

Peer-review under responsibility of the organizing committee of GHGT-13.

* Corresponding author. Tel.: +49-2461-614064; fax: +49-2461-616695.
E-mail address: l.zhao@fz-juelich.de

Keywords: CCS; post-combustion; membrane gas separation; heat exchanger; cooling

1. Introduction

Although the contribution of renewable energy technologies is growing significantly around the world, fossil fuels such as coal will remain central to the world's power supply for the next few decades. With the world's dependence on fossil fuels not expected to significantly abate in the short to medium term, carbon capture, and storage (CCS) presents itself as a critical technology to reducing CO₂ emissions and decarbonizing both the industrial and power sectors [1]. Three main routes have emerged as viable for capturing CO₂ from power plants: post-combustion, oxyfuel-combustion and pre-combustion [2]. Each has its pros and cons. In the near future, the post-combustion carbon capture process shows particular promise because of its ease of integration with existing coal-fired power plants [3]. Competing technologies for post-combustion carbon capture are absorption, adsorption, cryogenic fractionation and membrane-centered methods [2, 4].

Competing with chemical absorption, gas separation membranes used for post-combustion capture carry advantages in their potential for less environmental impact, since the solvent degradation leads to an additional burden for the environment. Furthermore, membrane modules can be used as add-on equipment with fewer modifications to power plants. The other potential advantage is that for low degrees of CO₂ separation, a stage-arranged membrane system demands a lower specific energy than that required for MEA absorption [5, 6]. Numerous groups and researchers around the world are involved in the material and process development of this approach [5, 7-22].

Although some processes [5, 13, 14] have been explored with consideration to their energetic and economic aspects, no detailed simulation about the cooling system for the membrane capture route has yet been performed. Since the membrane property is strongly influenced by the temperature, a thorough investigation of the entire system (capture and cooling) becomes significant for the future application.

In this paper, drawing on the in-house-developed cascaded membrane system [5, 23, 24], a further exploration of the capture and cooling system is carried out. An energetic comparison between membrane and chemical absorption is then expounded [25].

Aspen Plus is process simulation software widely used in research and industry. There are different thermodynamic models for the energy balance calculation; for the case described here, the Peng-Robinson equation of state with Boston-Mathias modifications (PR-BM) was used for the simulation. The Aspen Exchanger Design and Rating EDR is a tool for providing a technically and economically optimized shell-and-tube heat exchanger design for a given process conditions. A rigorous design of the cooling system will be held with the aid of EDR.

Nomenclature

$T_{h.in}, T_{h.out}$	hot stream's inlet and outlet temperature
$T_{c.in}, T_{c.out}$	cold stream's inlet and outlet temperature
\dot{m}_h, \dot{m}_c	mass flow rate of hot and cold stream
$c_{p,h}, c_{p,c}$	heat capacity of hot and cold stream
U	overall heat transfer coefficient
A	heat exchanger area
ΔT_m	logarithmic mean temperature difference
$\Delta T_1, \Delta T_2$	temperature difference $T_h - T_c$

2. Process and material description

2.1. Reference power plant

The Reference Power Plant Nord Rhine-Westphalia (RPP-NRW) [26] was used for the energetic analyses. After SCR-DeNO_x, dust removal (E-filter) and desulphurization (FGD), the flue gas has a pressure of approximately 1 atm and temperature of 50–70 °C.

A hard coal known as Klein Kopje was used to simulate the flow rate and the components of the flue gas. The element analysis data of Klein Kopje coal are: C 65.5%, H 3.5 %, O 7.4%, N 1.5%, S 0.6%, ash 14.2%, moisture 7.3%, while the heat value is 25 MJ/kg. The coefficient of air excess (air-to-fuel ratio) is assumed to be 1.15. The basic data of the RPP-NRW and simulation results of the flue gas are listed in Table 1. The residue of the pollutant in the flue gas consisted of approximately 50 vppm SO₂ and some 200 ppm NO₂.

Table 1. RPP-NRW power plant basic data [26] and simulation results of the flue gas conditions after removal of the pollutants using Klein Kopje hard coal

Power plant RPP-NRW	
Output gross	600 MW
Output net	555 MW
Net efficiency	45.9 %
Steam parameters	285 bar/600°C/620°C
Operation time	6000 h/year
Fuel input	1.0 Mt/year
Investment costs	517.1 million euro
O&M costs	7.8 million euro/year
Flue gas conditions after pollutants removal	
Pressure	1.05 bar
Temperature	50~70 °C
Flow rate	70670 Kmol/h
Flue gas component	Molar fraction [%]
CO ₂	13.5
N ₂	70.1
O ₂	3.7
H ₂ O	11.9
Ar	0.8

2.2. CO₂-selective membrane

Rubbery polymers based on PEO or PEG have emerged as promising candidate materials [27], drawing on the material selection guidelines proposed by Merkel et al. [14]. The feasibility of producing block copolymers such as Polyactive® [21, 28, 29] on a large scale is an important prerequisite for the subsequent fabrication of gas separation membranes and modules. Crosslinked PEO systems are promising for use in post-combustion carbon capture if the material design strategy can be extended to the fabrication of thin-film composite or asymmetric membranes. Based on data in the literature and from the Membrain [30], MetPore [31] and MemKoR [32] projects, the membrane properties in terms of temperature variation are listed in Table 2.

2.3. Cascaded membrane system

A scaled-up cascaded membrane system, as shown in Figure 1, is used for the process analysis. The first membrane (Mem 1) is driven by a vacuum pump (100 mbar) and the second (Mem 2) by a compressor (4 bar). The retentate of the second membrane is expanded and recycled as the feed of the first membrane. Part of the compression energy is then recovered by a turbo expander. The membrane cascade is located downstream of the flue gas cleaning processes and prior to the cooling tower.

Table 2. Membrane properties (permeance and selectivity) of Polyactive® membrane, referring to data from the literature [15, 21, 27-31], the unit for permeance is $\text{Nm}^3\text{m}^{-2}\text{h}^{-1}\text{bar}^{-1}$

Polyactive® membrane			
Temperature	50°C	30°C	25°C
CO ₂ permeance	5	4.3	3
H ₂ O permeance	15	43.3	53
CO ₂ /N ₂	25	36	50
O ₂ /N ₂	2.8	2.8	2.8
Ar/N ₂	2.8	2.8	2.8
SO ₂ /N ₂	270	270	270
NO/N ₂	5	5	5

A wet scrubber was adopted upstream of the membrane system, referring to a post-combustion process presented by Rheinisch-Westfälisches Elektrizitätswerk AG (RWE) [33]. This scrubber has two functions, one of which is the pollutant (SO_x, NO_x and dust) content of flue gas being further reduced, i.e., SO_x can be decreased to 10 vppm; the other is that flue gas can be further cooled down to 25 °C. The latter is a crucial factor for the membrane process, as the working temperature of the Polyactive® membrane strongly influences its performance [34].

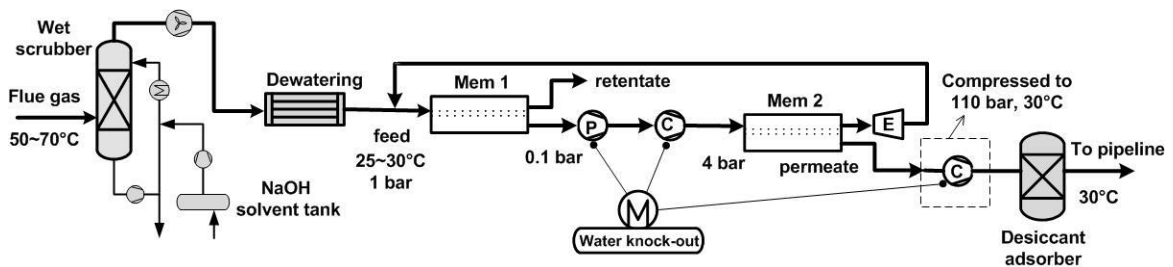


Figure 1. Schematic illustration of the scaled-up cascaded membrane system

The final CO₂ stream must be of a specific quality in order to meet the technical requirement for pipeline transport. Although maintaining the CO₂ molar fraction at no less than 95% is of greater priority in this work, according to Zhao et al. [23] the following requirements should also be met:

- 1) Water content should be equal to or lower than 500 ppm in order to prevent corrosion, hydrate formation and two-phase flow.
- 2) The concentration of contaminants, e.g., SO₂, H₂S and O₂, must be limited for reasons of safety.
- 3) The molar concentrations of non-condensable gases, such as: N₂, NO_x, CH₄, Ar and H₂ must be limited to below 4 mol% in total.

There are three ways of removing the water from flue gas in the CCS membrane system (see Figure 1), which are as follows:

- 1) Removal of water before the flue gas enters the capturing system. This can be achieved by dehydrating the SPEEK membrane by creating an H₂O partial pressure of 40 mbar when connected to a condenser [35]. Since this dehydrating process does not require extra energy, no additional energy consumption for this dehydration process need be considered.
- 2) Removal of water between compression stages in combination with intercooling.
- 3) Removal of small amount of water via desiccant after CO₂ separation and compression to ensure the water content in the end CO₂ product falls within the accepted limit.

Applying the dewatering process prior to CO₂ separation leads to lower energy consumption across the whole system [34].

2.4. Heat exchangers in the cooling system

Heat exchangers in a cascaded membrane system are classified into two categories according to their function and location, namely direct and indirect contact heat exchangers. The wet scrubber used in cooling the flue gas can be considered a direct contact heat exchanger, as shown in Figure 1. The other category is described as an indirect contact heat exchanger, namely an intercooler and preheater. The intercooler cools down the flue gas between compression machines, i.e., compressors and vacuum pumps, in order to dissipate the heat gained from the compression process. The preheater then consumes the heat gained from the intercoolers in order to heat up the flue gas before the latter enters the expander (see Figure 2).

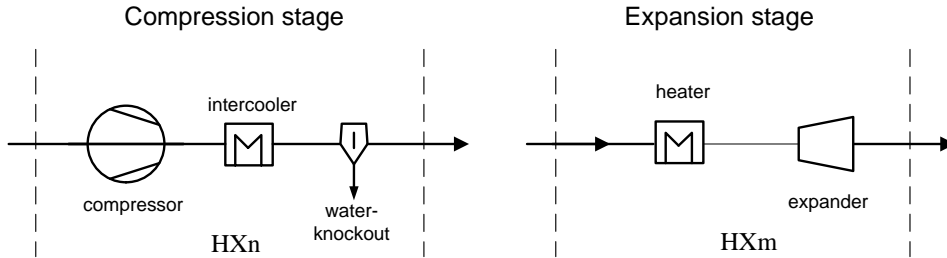


Figure 2. A schematic drawing of compression and expansion process components

Heat transfer is principally governed by the following equations:

$$\dot{Q} = \dot{m}_h c_{p,h} (T_{h.in} - T_{h.out}) \quad (1)$$

$$\dot{Q} = \dot{m}_c c_{p,c} (T_{c.out} - T_{c.in}) \quad (2)$$

$$\dot{Q} = U A \Delta T_m \quad (3)$$

Where ΔT_m is the logarithmic mean temperature difference and can be determined from the following equation:

$$\Delta T_m = \frac{(T_{h.in} - T_{c.out}) - (T_{h.out} - T_{c.in})}{\ln \left(\frac{T_{h.in} - T_{c.out}}{T_{h.out} - T_{c.in}} \right)} = \frac{\Delta T_1 - \Delta T_2}{\ln \left(\frac{\Delta T_1}{\Delta T_2} \right)} \quad (4)$$

Shell-and-tube heat exchangers are the most commonly used exchanger type in the process and petrochemical industry, accounting for more than 65% of the market share. Most of their advantages can be enumerated as follows: a) a compact, large heat transfer area in a small volume; b) mechanical stability to withstand high pressures; c) well-established design procedures; and d) ease of cleaning [36]. According to the design conditions in this work, it has been found to be more efficient to allocate the flue gas to the tube side and cooling/heating water to the shell side for the following reasons:

- 1) Corrosion: more corrosive fluid should be allocated to the tube-side, as this will reduce the exchanger cost by avoiding the use of anti-corrosion material on the shell-side.
- 2) Viscosity: a higher heat-transfer coefficient is obtained by allocating more viscous fluid to the shell-side.
- 3) Stream flow-rates: the fluid having the lowest flow rate should be allocated to the shell side in order to attain the most economical design [36].

The main components of the shell-and-tube include tubes, shells, nozzles, baffles and tube sheets, which are schematically illustrated in Figure 3 according to the Tubular Exchanger Manufacturers Association Inc. (TEMA) standards [37]. The standard TEMA shell-type BEM was selected for the following simulations.

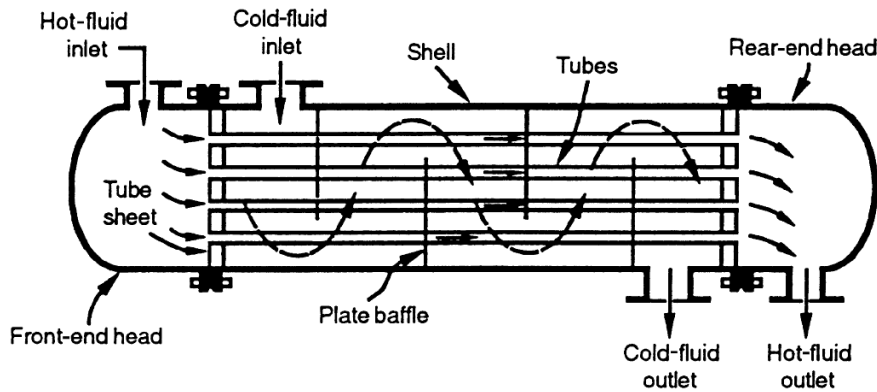


Figure 3. Shell-and-tube heat exchanger-type BEM from the TEMA standards [37]

The initial considerations assumed for the intercoolers and preheaters' preliminary design are shown in Table 3.

Table 3. Assumed parameters for the capture process

Parameter	Unit	Value
Cooling water pressure	bar	3
Cooling water temperature	°C	15
Polytropic efficiencies of compressors and vacuum pumps	%	85
Isentropic efficiency of expanders	%	85
Hot stream pressure drop in each heat exchanger	mbar	30

Shellside design

The shellside calculations are far more complex than those for the tubeside, largely because on the shellside there is not only one flow stream, but one principal cross-flow stream and four leakage or bypass streams. There are various shellside flow arrangements, as well as various tube layout patterns and baffling designs, which together determine the shellside stream analysis [38].

Tube layout patterns

There are four tube layout patterns, as shown in Figure 4: triangular (30°), rotated triangular (60°), square (90°) and rotated square (45°). A triangular (or rotated triangular) pattern will accommodate more tubes than a square (or rotated square) pattern. Furthermore, a triangular pattern produces high turbulence and therefore a high heat-transfer coefficient [38].

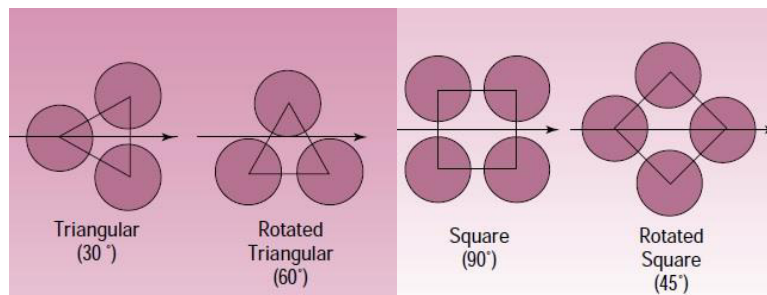


Figure 4. Tube layout patterns [38]

Baffling

Baffles are used to support tubes, enable a desirable velocity to be maintained for the shellside fluid, and prevent the failure of tubes due to flow-induced vibration. There are two types of baffles, namely: plate and rod. Plate baffles may be single-segmental, double-segmental or triple-segmental, as shown in Figure 5 [38].

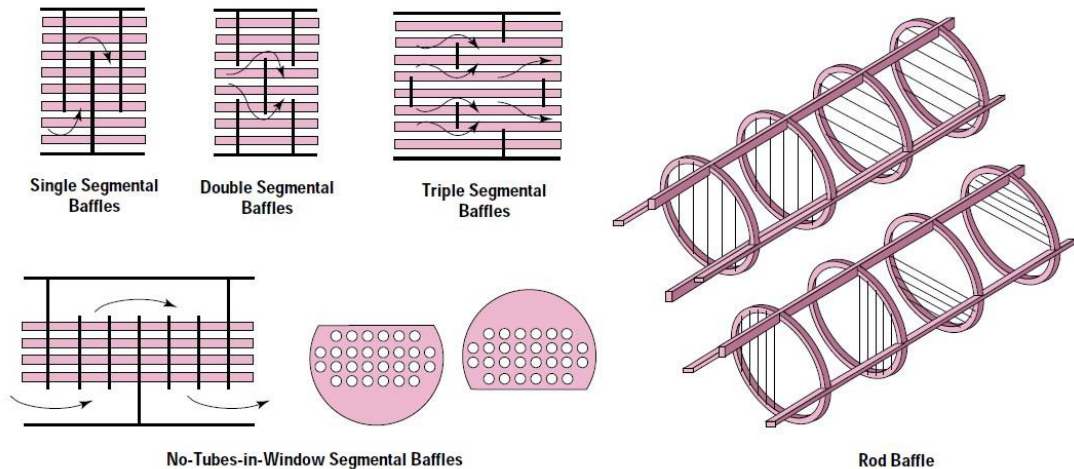


Figure 5. Types of baffles [38]

The Aspen Exchanger Design and Rating (EDR) is a tool for providing a technically and economically optimized shell-and-tube heat exchanger design for given process conditions. To achieve a rigorous design, design, rating and simulation should be completed in sequence [25].

- **Design:** The first step is to input all process conditions, pressures, temperatures, stream species and expected heat duties. If the design is successful, the proposed exchanger geometry can then be tested in the rating step.
- **Rating:** If the design succeeds, the design recommends a specific geometry for the exchanger; e.g., size and number of shells, size and number of tubes, number of baffles and spacing. The proposed design shall then be rated to evaluate it and discuss its adequacy in achieving temperatures and pressures within the predefined limitations.
- **Simulation:** If the design is successfully rated, the EDR input file will be integrated into the simulation model to observe the entire capture system's behaviour.

The inlet pressures and temperatures, stream components and exchanger heat duty from the preliminary design were used as inputs in the EDR input file.

3. Results and discussion

3.1. Influence of working temperature

As Table 2 indicates, it is clear that working temperature significantly influences the membrane property. If a comparison of between 50 °C and 25 °C working temperatures is considered, the latter has an energetic advantage as well as higher CO₂ purity than the former at a given degree of separation [27]. These results are shown in Figure 6. The ideal gas means that the flue gas is only composed of 14 mol% CO₂ and 86 mol% N₂ [5]; in this case, the membrane CO₂/N₂ selectivity was assumed to be the same as that of the membrane working at 30 °C. The curve of MEA absorption was obtained within the framework of the MetPore project [31], in which the feed flue gas has the same boundary condition as that for membrane capture. The absorber is operated at 45 °C and 1 bar, and the stripper works at 120 °C. It should be mentioned here that the pressure drop in coolers and heaters was neglected. On the basis of the above outcomes, it can be known that for an energy-efficient membrane capture system, the cooling

process is very important and will be investigated in detail in the following.

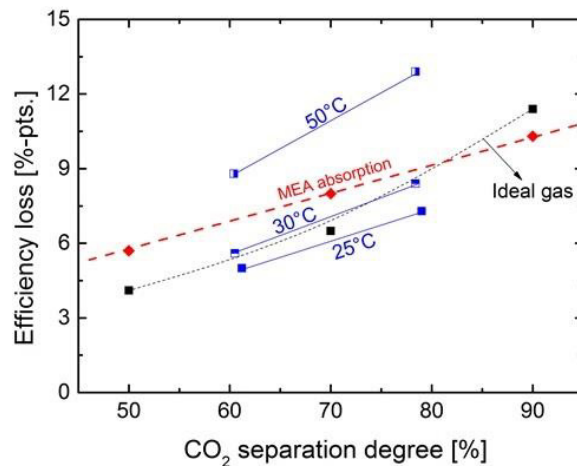


Figure 6. Influence of membrane working temperature on the efficiency loss of a membrane capture system

3.2. Flue gas pre-cooling

After FGD, the flue gas has a temperature of 50-70 °C prior to the membrane process. In order to ensure that the membrane works at 25 °C with the best property for CO₂ separation, flue gas pre-cooling should be carried out.

The wet scrubber in the MEA absorption technology is assumed to also be suitable for membrane separation [33]. It is used as secondary flue gas desulphurization equipment, because remaining SO₂ traces from the FGD plant can still cause MEA solvent degradation. Although SO₂ is not considered a feed gas component in this simulation, the reduction of SO_x helps decrease the corrosion problem in the capture process.

A simple model was built to investigate the amount of cooling water flow rate needed to reach 25 °C prior to the first membrane. As demonstrated in Figure 7, 50 and 70 °C inlet feed gas temperatures were considered in this investigation. The flue gas flow rate is 70670 kmol/h. The required cooling water mass flow rates are about 7000 and 9000 ton/h, respectively. Consequently, these extra costs for both equipment and water should be considered in the economic evaluation of the capture process and in the future industrial applications.

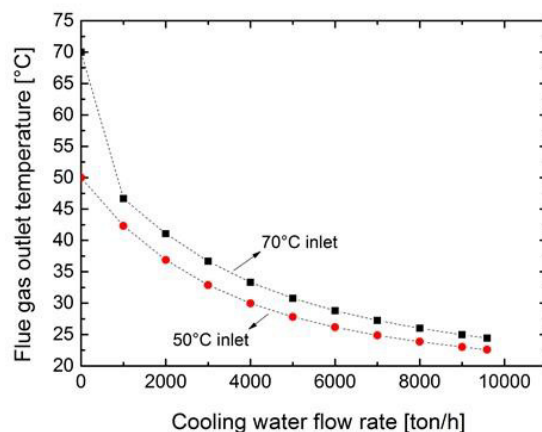


Figure 7. The effect of the amount of cooling water flow rate on flue gas temperature in a direct contact pre-cooler

3.3. Dewatering prior to CO₂ separation

As discussed in Section 2.3, in addition to CO₂ separation, water removal from flue gas is also an important topic that should be investigated in detail. A study for a 70% degree of CO₂ separation was carried out in our previous paper [23].

The working temperature of the membrane was assumed to be 25 °C. In the simulation, a flash unit was placed in order to get rid of the condensed water. A SPEEK membrane [35] was then applied for water removal and situated prior to the CO₂ membrane. Three water-removing options were explored for both 50% and 70% degrees of CO₂ separation, namely: a) no removal of water; b) one-third removal of water; and c) two-thirds removal of water.

The positive sweep effect from improving the degree of CO₂ separation was monitored; when using the same membrane area, the degree of CO₂ separation increases. A comparison of efficiency loss amongst ideal flue gas, no dewatering, 1/3 dewatering, 2/3 dewatering and MEA absorption is schematically illustrated in Figure 8. The 2/3 water-removal option shows energetic significance compared to no-dewatering and 1/3 dewatering, as does MEA absorption; 2/3 water removal will be considered for further simulations in which heat exchangers are integrated into the system.

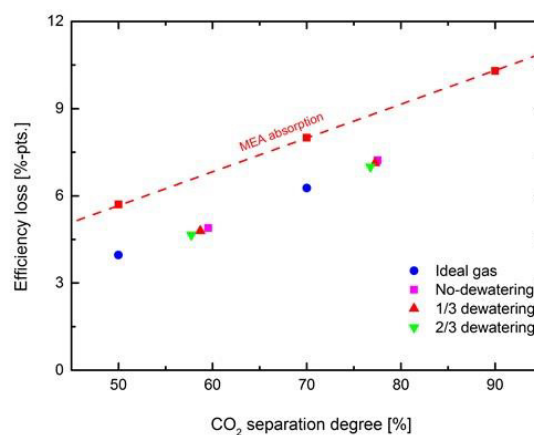


Figure 8. Influence of water content on degree of separation and energy consumption compared to MEA absorption

3.4. Heat exchanger preliminary design

For vacuum pump and compressor

According to the work of Ek Weis [39], the 2-stage vacuum pump approach in the capture section has not proven successful in reaching a flue gas temperature of 25 °C prior to the inlet of the second membrane. However, a four-stage vacuum with inter-cooling between stages (see Figure 2, compression stage), namely HX1 to HX4 and a two-stage compressor with intercooling, namely HX5 and HX6, were sufficient to reach the desired temperature [25]. In this paper, a 25 °C flue gas temperature must be achieved in order to reach the high CO₂/N₂ selectivity at this temperature range. Then, for the HX6, the flue gas outlet temperature is the most important parameter for process development. In this section, the heat exchanger design is based on the case of 50% degree of CO₂ separation.

From Table 4, it can be deduced that a 30 kg/s cooling water mass flow rate and a temperature difference of 21.5K meets the required hot stream outlet temperature within the range of 25-30°C. The temperature difference of 21.5K is the minimum possible value to simultaneously reach the desired hot stream outlet temperature while not violating the minimum limit of 5K temperature difference at pinch point, which is demonstrated in Figure 9. The non-linear behaviour of the hot stream (flue gas) is due to the condensation of water vapour in flue gas, i.e., phase change. The assigned mass flow rate of 30 kg/s will be applied for the rest of the heat exchangers in the compression

section of the capture part. The same strategy applied for a temperature difference at HX6 will then be applied for the rest of heat exchangers, from HX1 to 5.

Table 4. HX6 design approach

Heat Exchanger 6 (HX6)			
Cooling water flow rate [kg/s]	$T_{h,in} - T_{c,out}$ [K]	Hot stream outlet temperature [°C]	Cold stream outlet temperature [°C]
10	5	60.5	91.3
20	5	34.2	91.2
30	21.5	26.4	75.3

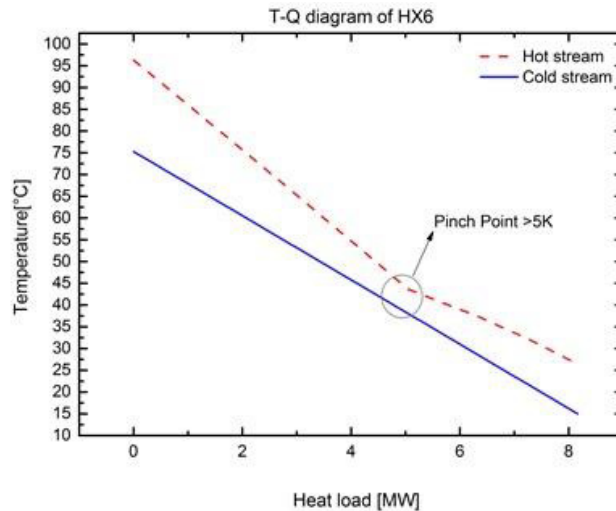


Figure 9. T-Q Diagram of HX6 at 30 kg/s coolant flow rate and $\Delta T (T_{h,in} - T_{c,out})$ of 21.5K

In order to assign U values (overall heat transfer coefficient) that are relatively close to the actual values, heat exchanger states have been classified into three different categories according to the working fluid, i.e., hot stream temperature, pressure and whether condensation occurs inside the exchanger.

After assigning the previous average overall heat transfer coefficient values in Table 5, the following required heat transfer surface area (see Table 6) can be calculated, according to equation 3, using the Aspen Plus heat exchanger shortcut design.

For expander

The heat recovered from intercooling between compression stages has raised the cooling water to a temperature of 65 °C and has proved to be sufficient to raise the temperature of flue gas in the preheaters to 63 °C before entering the expanders. The following graphs (Figure 10) show the heat duty and temperatures of the hot stream, i.e., hot water, and the cold stream, i.e., flue gas, at both preheaters are located before each expansion process (see Figure 2, expansion stage).

Table 5. Average U values for heat exchangers at different hot stream conditions [40, 41]

Hot Stream Pressure Range	Condensation	Overall Heat Transfer Coefficient [W/m^2K]
Below/equal atmospheric pressure	No	65
Below/equal atmospheric pressure	Yes	150
Above atmospheric pressure	Yes	300

Table 6. Surface area estimates for intercoolers in the capture section

Heat exchanger	Average heat transfer coefficient [W/m ² K]	Surface Area [m ²]
HX1	65	4770
HX2	65	5015
HX3	65	4907
HX4	150	4435
HX5	300	2553
HX6	300	2970

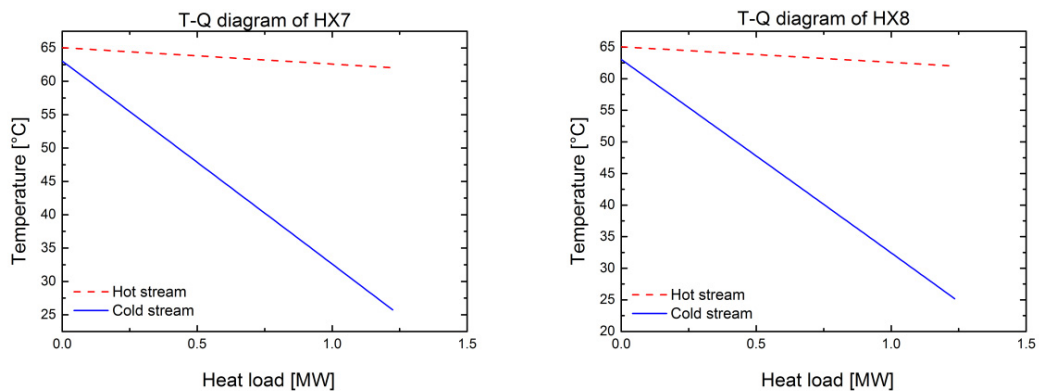


Figure 10. T-Q diagrams of preheaters in expansion system

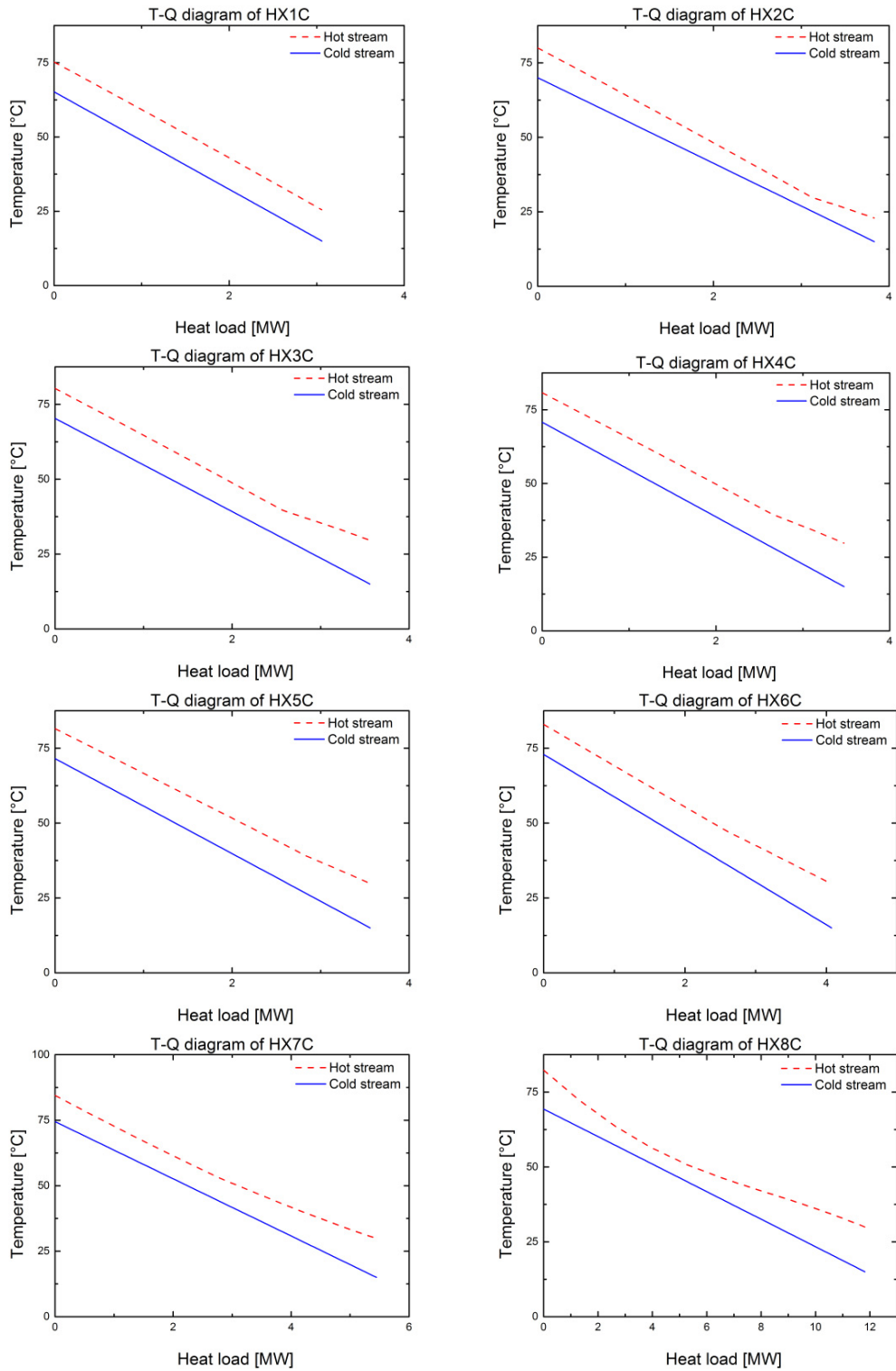
As shown in the T-Q diagrams in Figure 10, the amount of heat duty needed is extremely low compared to the intercoolers case, which is logical given that the heat transfer coefficient of saturated liquid water causes the heating fluid to always be considerably hotter than the heating flue gas [42], which means an much lower surface area is required to reach a ΔT ($T_{h.in} - T_{c.out}$) of 2K. It is also important to mention the relatively high water flow rate, since the same amount of water used in the cooling operation is fed to the preheaters and the water flow rate per preheater is three times that of an intercooler (see Table 7).

Table 7. Heating water flow rates, U value and ΔT ($T_{h.in} - T_{c.out}$) for each heat exchanger on the expansion side of capture system

Heat exchanger	Heating water flow rate [kg/s]	Average heat transfer coefficient [W/m ² K]	ΔT ($T_{h.in} - T_{c.out}$) [K]	Surface Area [m ²]
HX7	90	300	2	346
HX8	90	300	2	346

For the CO₂ compressor

An eight-stage compression system was applied to deliver the end product CO₂ at 110 bar and 30 °C [25]. The strategy used in capture section was then applied in the compression section to determine the temperature difference ($T_{h.in} - T_{c.out}$) and cooling water flow rate required to reach the desired output conditions without thermodynamic violations. The temperature difference and water mass flow rate was calculated to be 10K and 19.3 kg/s, respectively. The T-Q diagrams for the eight heat exchangers from HX1C to 8C in the CO₂ compression section are shown in Figure 11.

Figure 11. T-Q diagrams of heat exchangers in the CO₂ compression section

The U value of 300 W/m² K was assigned according to the classification in Table 5 and the following surface areas in Table 8 were calculated using Aspen Plus. (A parallel paper is being prepared to integrate the exhaust heat from the CO₂ compression process with the water-steam cycle of the reference power plant).

Table 8. Surface areas of heat exchanger intercoolers for CO₂ compression

Heat exchanger	Average heat transfer coefficient [W/m ² K]	Surface Area [m ²]
HX1C	300	975.6
HX2C	300	1829.5
HX3C	300	1154.4
HX4C	300	1034.1
HX5C	300	1014.1
HX6C	300	1202.1
HX7C	300	1812.6
HX8C	300	4836.6

3.5. Aspen EDR design

On the vacuum pump side

The heat exchangers in this part of the system share the same operating conditions, as the flue gas pressure is within the vacuum level, which means less heat transfer coefficient of the flue gas stream, as the pressure drop is therefore low [43]. In the design phase, certain parameters are essential in order to enhance the heat transfer efficiency and control the pressure drop on both the shell and tube sides. These parameters have been configured as follows:

- **Baffle type:** The single-segmental baffle type is the default setting in EDR. The double-segmental configuration has proven to decrease the pressure drop across the shell-side compared to the other streams' fractions, and hence increases the thermal efficiency of the exchanger.
- **Tube pattern:** The tube pattern also has a major influence on both heat transfer and pressure drop on the shell-side. The 30° tube pattern is the default tube pattern in EDR, while the 45° pattern has been found to be the most suitable, together with the double-segmental baffle type. Another effect that should be mentioned is the pressure drop on the tube-side, since the compactness of the heat exchanger, i.e., the number of tubes inside the shell, decreases from the 30° to the 90° tube pattern, while the pressure drop also decreases as the number of tubes per shell unit does [44].

The following figures, Figure 12 and Figure 13, describe the common structural features of shell type, baffle type and tube pattern shared among heat exchangers in this section. The dimensions, however, belong to the first heat exchanger HX1.

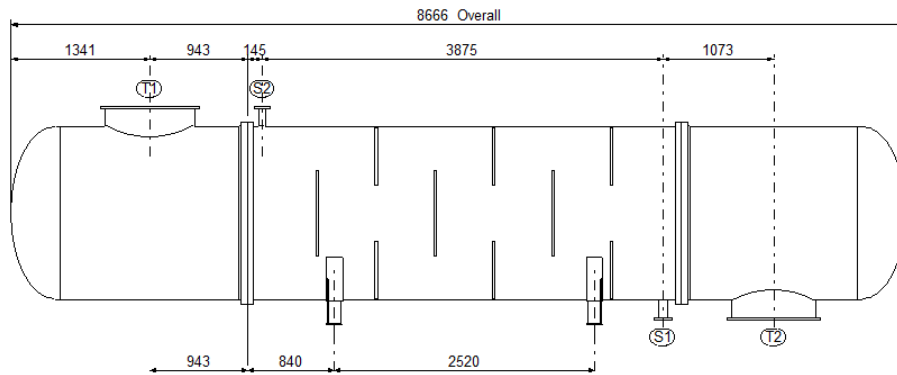


Figure 12. Front view of an HX1 structure provided by the Aspen-EDR tool

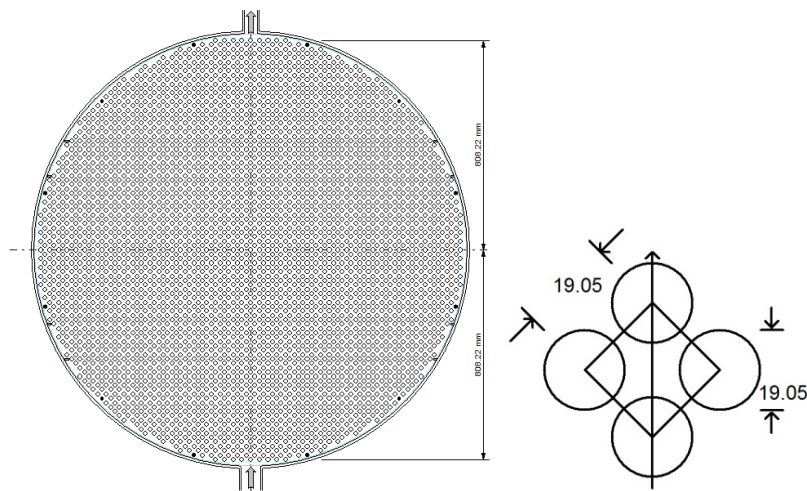


Figure 13. Side view of the tube bundle and tube pattern of the HX1, provided by the Aspen-EDR tool

On the compressor side

Due to the operating pressures of flue gas in this section of about 2-4 bar for the HX5 and HX6, respectively, the heat transfer coefficient on the flue gas side is relatively higher than the vacuum pump section. Heat transfer is, therefore, a lesser problem in this case and a more compact heat exchanger design approach, which reduces the cost as fewer shells are needed, is to be preferred.

- **Baffle type:** The baffle type considered in this case is the same as the previous group of heat exchangers, namely double-segmental (see Figure 14).
- **Tube pattern:** In this case, the default 30° tube pattern has been approved by Aspen-EDR with regard to thermal efficiency. This can be understood due to the lower accompanying costs, as a lower number of shells will be required due to the greater number of tubes per shell (see Figure 15).

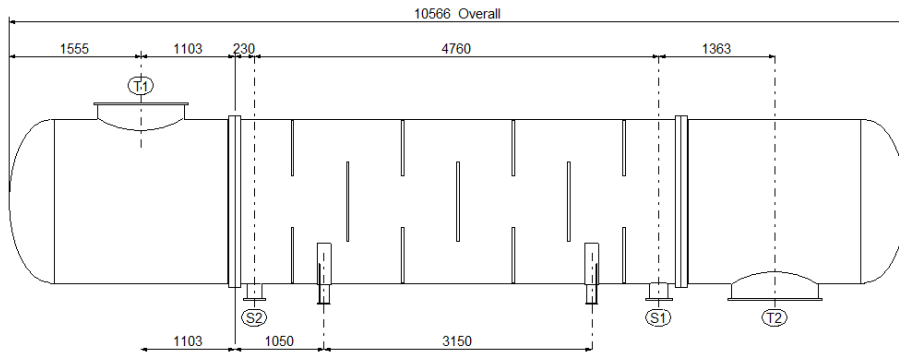


Figure 14. Front view of the HX5 structure provided by the Aspen-EDR tool

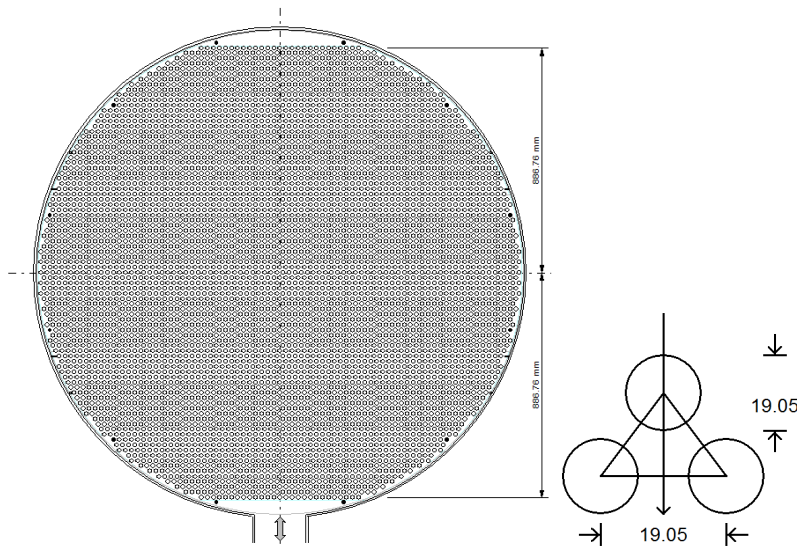


Figure 15. Side view of the tube bundle and tube pattern of the HX5 provided by the Aspen-EDR tool

On the expander side

As illustrated in Table 7, the cooling water mass flow rate per exchanger on this side is relatively high compared to exchangers on the cooling side. This has caused a vibration problem that has been identified by Aspen-EDR during the design phase at the inlet and outlet nozzles of the shell and in the tubes.

This design problem has been solved using three approaches. First, the water flow rate was halved by splitting each preheater into two heat exchangers in parallel. Secondly, as suggested by Thulukkanam [45], in order to make the tubes more rigid, the length of span between baffles should be as low as possible in order to develop a higher natural frequency. Thirdly, the tube pattern should provide the lowest possible pressure drop across the shell-side in order to decrease the fluid velocity at the inlet and outlet nozzles.

The afore-mentioned approaches can be translated into the following design considerations.

- **Baffle type:** Since the goal is to minimize the span between baffles, the number of baffles within a unit shell should be increased. The double-segmental baffle has not proven itself capable of achieving the minimum span required. The triple-segmental was, however, successful in preventing vibration within the tubes (see Figure 16).

- **Tube pattern:** Since the pressure drop across the shell-side decreases from the 30° to the 90° tube pattern, it was essential to investigate different tube patterns and their effect on pressure drops and hence the water velocity at the inlet and outlet nozzles. The 90° tube pattern has been successful in achieving this goal (see Figure 17).

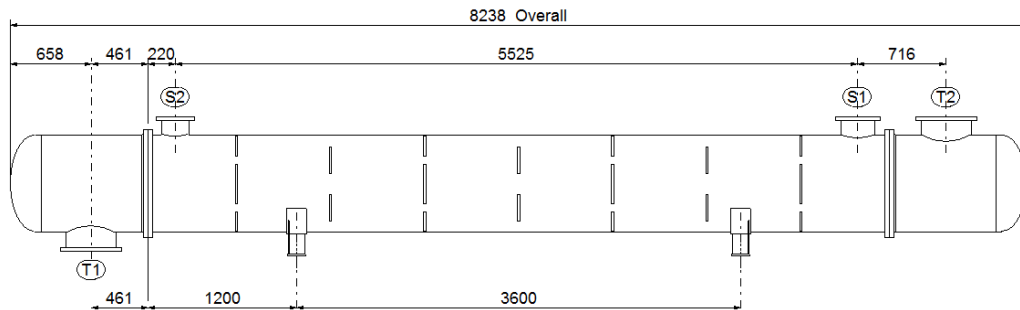


Figure 16. Front view of the HX7 structure provided by the Aspen-EDR tool

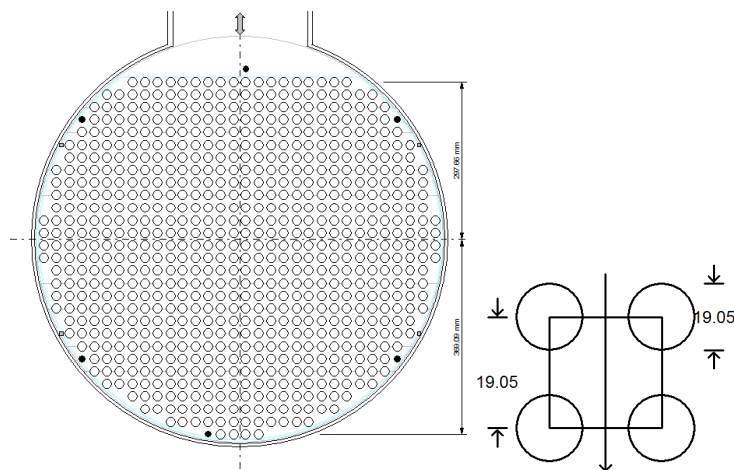


Figure 17. Side view of the tube bundle and tube pattern of the HX7 provided by the Aspen-EDR tool

3.6. Integrating the heat exchanger EDR design with the cascaded membrane system

The simulation results of the heat exchangers are listed in Table 9 and Table 10 for 57% and 76% degrees of CO₂ separation, respectively. In comparison to the data shown in Table 6 and Table 9, it is known that EDR simulation contributes to a higher demand for surface area. The reason for this is that the overall heat transfer coefficient of the EDR design is lower than that for the preliminary design. The pressure drop in each heat exchanger with the EDR design is higher than the assumed 30 mbar. For the HX4, HX5 and HX6, the value is almost 8-11 times larger than 30 mbar.

In order to compensate for the pressure drop in the cooling process, the pressure ratio is recalculated and listed in Table 11, whose values were determined by the design spec feature in Aspen Plus to maintain the outlet pressure from each heat exchanger at the same level as the preliminary design case.

The higher pressure ratios, compared with the preliminary design case, required compression machines to overcome the new pressure drops in the heat exchangers, leading to an increase in the system's energy consumption. The specific energy consumptions of 57% and 76% degrees of CO₂ separation are 265.8 and 313.7 kW per ton of CO₂, resulting in the efficiency loss of 5.3 and 8.3 percentage points, respectively. The effect of the rigorous heat exchanger design on the system's energy penalty for 57% and 76% degrees of CO₂ separation, compared with the

MEA energy penalty, is described in Figure 18.

One point to be noted is that chemical absorption has also been improved in the last period through the use of new solvents. Specific energy consumption has thereby significantly decreased to 2700 MJ/t_{CO₂}, previously 3500 MJ/t_{CO₂} [6]. Thus, to enable the membrane capture process to better compete against the absorption method, a further investigation should be carried out to integrate the exhaust heat from the CO₂ compression process with the water-steam cycle, which will be presented in a parallel paper.

Table 9. Stream results of heat exchangers in the capture system by Aspen-EDR for 57% degree of CO₂ separation

Heat exchanger	HX1	HX2	HX3	HX4	HX5	HX6	HX7	HX8
Surface area (effective) per unit [m ²]	6356	5185	3834	3966	3447	3553	243	243
Baffle type (x-segmental)	Double	Double	Double	Double	Double	Double	Triple	Triple
Tube pattern	45	45	45	45	30	30	30	30
Pressure drop in tube-side [mbar]	72	82	88	322	270	284	39	39
Overall heat transfer coefficient (dirty) [W/m ² K]	52	66	88	199	220	242	189	189
Flue gas T _{in} [°C]	109.2	109.4	104.1	116.1	103.9	101.5	25.9	25.9
Flue gas T _{out} [°C]	28.9	28.6	25.8	28.7	30.9	25.9	75.5	75.5

Table 10. Stream results of heat exchangers in the capture system by Aspen-EDR for 76% degree of CO₂ separation

Heat exchanger	HX1	HX2	HX3	HX4	HX5	HX6	HX7	HX8
Surface area (effective) per unit [m ²]	13878	10293	8225	8287	6403	7933	508	508
Baffle type (x-segmental)	Double	Double	Double	Double	Double	Double	Triple	Triple
Tube pattern	45	45	45	45	30	30	90	90
Pressure drop in tube-side [mbar]	72	84	77	249	257	345	77	77
Overall heat transfer coefficient (dirty) [W/m ² K]	49	65	75	157	223	278	279	279
Flue gas T _{in} [°C]	100	99.6	100	104	100	103	29.4	29.4
Flue gas T _{out} [°C]	24.5	24.75	24.71	23.17	25.13	26.27	62.7	62.7

Table 11. Primary and modified pressure ratios of compression/expansion machines in the capture system for 57% and 76% of CO₂ separation

Compression/Expansion machine	Primary pressure ratio	Modified pressure ratio for a 57% separation degree	Modified pressure ratio for a 76% separation degree
Vacuum pump 1	1.942	2.358	2.36
Vacuum pump 2	1.942	2.264	2.269
Vacuum pump 3	1.942	2.149	2.108
Vacuum pump 4	1.942	2.488	2.352
Compressor 1	2.023	2.264	2.251
Compressor 2	2.023	2.149	2.169
Expander 1	0.585	0.518	0.617
Expander 2	0.585	0.58	0.58

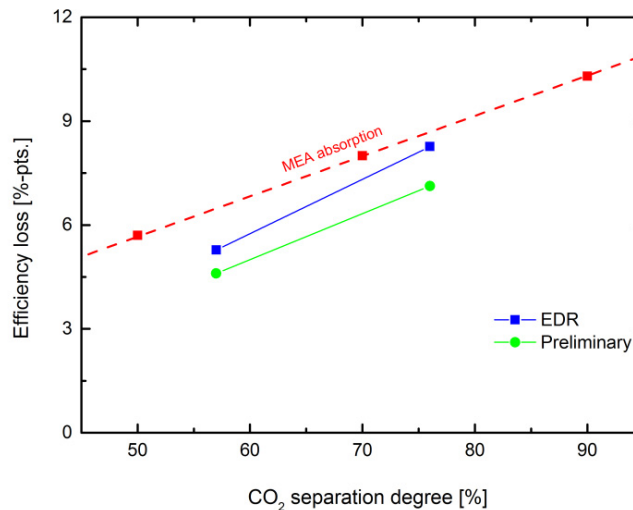


Figure 18. Comparison between EDR design and preliminary design regarding the system's efficiency loss

4. Conclusions

This paper investigates the design and influence of the machinery and equipment entailed by a gas separation membrane system for separating CO₂ from the flue gas emitted by the reference coal-fired power plant RPP-NRW. The investigation intended to simulate real flue gas and the performance of the system, and to evaluate the system's energy consumption accordingly.

Owing to the influence of working temperature on the membrane capture process, a cooling system was developed to cool the flue gas down to 25 °C, so that the membrane can reach a high degree of selectivity and decrease the energy consumption of the capture process.

The results have shown that the water content of real flue gas increases the energy consumption of the system compared to ideal flue gas containing only N₂ and CO₂. The water content, however, increases the degree of CO₂ separation, which is highly advantageous due to its positive sweep effect.

The removal of water from flue gas prior to capture has proved to reduce the system's energy consumption. A water removal ratio of 2/3 was adopted, as it provided the lowest energy penalty, with 4.7% and 7% for degrees of CO₂ separation of 58% and 77%, respectively, while still maintaining a considerably high separation degree.

The implementation of a rigorous heat exchanger design in the capture section showed new pressure drop values that exceed the pre-assumed value of 30 mbar by 3-11 orders of magnitude. This increase in pressure drop has resulted in a higher energy consumption and hence higher energy penalty.

The energy penalty of the membrane system for 57% and 76% degrees of CO₂ separation has been increased from 4.7%-pts to 5.3%-pts and 7%-pts to 8.3%-pts, respectively, after implementing the rigorous heat exchanger design. The values of the energy penalty, however, still haven't exceeded that of MEA absorption, assuming the vacuum pump's efficiency to be 85%.

In order to keep membrane separation processes competitive against chemical absorption, a further investigation to integrate the exhaust heat from the CO₂ compression process with the water-steam cycle of the power plant should be carried out.

Acknowledgements

Financial support from the MemKoR project (funding identifier: 03ET7064B), funded by the Federal Ministry of Economics Affairs and Energy (BMWi), Germany, within the framework of the COORETEC program, is gratefully acknowledged.

References

- [1] Tracking Clean Energy Progress, 2012, http://www.iea.org/media/etp/tracking/Tracking_Clean_Energy_Progress.pdf, last accessed on 25th August 2016.
- [2] Metz, B., et al., IPCC Special Report on Carbon Dioxide Capture and Storage, 2005, Cambridge University Press: United Kingdom & New York, USA, available in full at www.ipcc.ch.
- [3] Wang, M., et al., Post-combustion CO₂ capture with chemical absorption: A state-of-the-art review. *Chem. Eng. Res. Des.*, 2011. 89(9): p. 1609-1624.
- [4] Post-Combustion CO₂ Control, U.S. Department of Energy, <http://www.netl.doe.gov/research/coal/carbon-capture/post-combustion>, last accessed on 25th August, 2016.
- [5] Zhao, L., et al., Multi-stage gas separation membrane processes with post-combustion capture: energetic and economic analyses. *Journal of Membrane Science*, 2010. 359: p. 160-172.
- [6] Brinkmann, T., et al., Investigating the influence of the pressure distribution in a membrane module on the cascaded membrane system for post-combustion capture. *International Journal of Greenhouse Gas Control*, 2015. 39: p. 194-204.
- [7] Bounaceur, R., et al., Membrane processes of post-combustion carbon dioxide capture: A parametric study. *Energy*, 2006. 31(14): p. 2220-2234.
- [8] Favre, E., Carbon dioxide recovery from post-combustion processes: Can gas permeation membranes compete with absorption? *Journal of Membrane Science*, 2007. 294(1-2): p. 50-59.
- [9] Car, A., et al., PEG modified poly(amide-b-ethylene oxide) membranes for CO₂ separation. *Journal of Membrane Science*, 2008. 307(1): p. 88-95.
- [10] Follmann, P.M., et al., CO₂ separation via the post-combustion process with membranes in coal power plants. *Efficient Carbon Capture for Coal Power Plants*, ed. D. Stolten and V. Scherer 2011: Wiley_VCH Verlag GmbH & Co. KGaA. 381-401.
- [11] Ho, M.T., G.W. Allinson, and D.E. Wiley, Reducing the Cost of CO₂ Capture from Flue Gases Using Membrane Technology. *Ind. Eng. Chem. Res.*, 2008. 47: p. 1562-1568.
- [12] Deng, L., T.J. Kim, and M.-B. Hägg, Facilitated transport of CO₂ in novel PVAm/PVA blend membrane. *Journal of Membrane Science*, 2009. 340(1-2): p. 154-163.
- [13] Hussain, A. and M.-B. Hägg, A feasibility study of CO₂ capture from flue gas by a facilitated transport membrane. *Journal of Membrane Science*, 2010. 359: p. 140-148.
- [14] Merkel, T.C., et al., Power plant post-combustion carbon dioxide capture: An opportunity for membranes. *Journal of Membrane Science*, 2010. 359: p. 126-139.
- [15] Brinkmann, T., T. Wolff, and J.-R. Pauls. Post-Combustion Processes Employing Polymeric Membranes. in 2nd International Conference on Energy Process Engineering Efficient Carbon Capture for Coal Power Plants. 2011. 20th-22nd, 2011, Frankfurt am Main, Germany.
- [16] Teruhiko Kai, et al., Development of commercial-sized dendrimer composite membrane modules for CO₂ removal from flue gas. *Sep. Purif. Technol.*, 2008. 63(3): p. 524-530.
- [17] Powell, C.E. and G.G. Qiao, Polymeric CO₂/N₂ gas separation membranes for the capture of carbon dioxide from power plant flue gases. *Journal of Membrane Science*, 2006. 279(1-2): p. 1-49.
- [18] Lin, H. and B. Freeman, Materials selection guidelines for membranes that remove CO from gas mixtures. *Journal of Molecular Structure*, 2005. 739(1-3): p. 57-74.
- [19] Reijerkerk, S.R., et al., Poly(ethylene glycol) and poly(dimethyl siloxane): Combining their advantages into efficient CO₂ gas separation membranes. *Journal of Membrane Science*, 2010. 352(1-2): p. 126-135.
- [20] Car, A., et al., Tailor-made polymeric membranes based on segmented block copolymers for CO₂ separation. *Advanced Functional Materials*, 2008. 18: p. 2815-2823.
- [21] Yave, W., et al., Design, synthesis, characterization and optimization of PTT-b-PEO copolymers: A new membrane material for CO₂ separation. *Journal of Membrane Science*, 2010. 362(1-2): p. 407-416.
- [22] Sholes, C.A., S.E. Kentish, and G.W. Stevens, Effect of Minor Components in Carbon Dioxide Capture Using Polymeric Gas Separation Membranes. *Separation & Purification Reviews*, 2009. 38: p. 1-44.
- [23] Zhao, L., et al., Cascaded Membrane Processes for Post-Combustion CO₂ Capture. *Chemical Engineering & Technology*, 2012. 35(3): p. 489-496.
- [24] Zhao, L., et al., Concepts and investment cost analyses of multi-stage membrane systems for carbon dioxide recovery in post-combustion processes. *Energy Procedia*, 2009. 1: p. 269-278.
- [25] Abdelall, S., Investigation of turbo-machinery and heat exchangers in a membrane post-combustion system for CO₂ capture, in Master thesis 2013, Aachen University of Applied Sciences Jülich Division.
- [26] Konzeptstudie: Referenzkraftwerk Nordrhein-Westfalen (RWK NRW), February 2004, VGB Power Tech e.V., Essen, Germany.
- [27] Low, B.T., et al., A parametric study of the impact of membrane materials and process operating conditions on carbon capture from humidified flue gas. *Journal of Membrane Science*, 2013. 431: p. 139-155.
- [28] Yave, W., et al., CO₂-Philic Polymer Membrane with Extremely High Separation Performance. *Macromolecules*, 2010. 43(1): p. 326-333.
- [29] Yave, W., A. Car, and K.V. Peinemann, Nanostructured membrane material designed for carbon dioxide separation. *Journal of Membrane Science*, 2010. 350: p. 124-129.

- [30] Membrain, Oct. 2007 - Jun. 2011, MEM-BRAIN Alliance (Gas separation membranes for zero-emission fossil power plants), 18 research institutions and 5 industrial partners Coordinator: IEK-1, Forschungszentrum Jülich GmbH.
- [31] Metpore, Jan. 2007 - May. 2014, METPORE (Nano-structured Ceramic and Metal Supported Membranes for Gas Separation), funded by the Federal Ministry of Economics and Technology (BMWi), Germany.
- [32] MemKoR, Jan. 2016 - Dec. 2018, Membranverfahren für die Abtrennung von Kohlendioxid aus Kraftwerksrauchgasen, funded by the Federal Ministry of Economics and Technology (BMWi), Germany.
- [33] Peters, M. and S. Wallus. Dream Production - Chemical Utilisation of CO₂. Achema Tagung, Frankfurt am Main June 18, 2012.
- [34] Zhao, L., M. Weber, and D. Stolten, Comparative Investigation of Polymer Membranes for Post-combustion Capture. *Energy Procedia*, 2013. 37: p. 1125-1134.
- [35] Sijbesma, H., et al., Flue gas dehydration using polymer membranes. *Journal of Membrane Science*, 2008. 313: p. 263-276.
- [36] Coulson, J.M. and J.F. Richardson, *Chemical engineering*. Oxford: Pergamon Press.
- [37] TEMA Designation, http://www.engineeringpage.com/heat_exchangers/tema.html, last accessed on 25th August 2016.
- [38] Mukherjee, R., *Effectively Design Shell-and-Tube Heat Exchangers*. Chemical Engineering Progress, 1998. February.
- [39] Ek Weis, D., Investigation of CO₂ avoidance behaviour of membrane capture in post combustion processes, in Department of Energy and Environment 2011, Chalmers University of Technology Göteborg, Sweden
- [40] Kuhn, S., et al., Wärmetauscher zur Abwärmenutzung, in IKARUS Instrumente für Klimagas-Reduktionsstrategien 1994, Münzer Kuhn Leis Ingenieurgesellschaft mbH, München.
- [41] Coulson, J.M. and J.F. Richardson, *Chemical engineering*, in Chemical engineering., Pergamon Press.: Oxford. p. 83.
- [42] Annaratone, D., *Engineering Heat Transfer 2010*: Springer Berlin Heidelberg.
- [43] Hesselgreaves, J.E., *Compact heat exchangers : selection, design and operation* / John E. Hesselgreaves. %U <http://wwwzb.fz-juelich.de/contentenrichment/inhaltsverzeichnisse/bis2009/ISBN-0-08-042839-8.pdf>2001, Amsterdam: Pergamon Press. XVIII, 398 S.
- [44] Shah, R.K. and D.P. Sekulic, *Fundamentals of heat exchanger design* / Rsmesh K. Shah ; Dusan P. Sekulic, 2003, Wiley: New York, p. 12-47.
- [45] Thulukkanam k., Flow-Induced Vibration of Shell and Tube Heat Exchangers, in *Heat Exchanger Design Handbook*, Second Edition 2013, CRC Press. p. 509-562.